High-fidelity Event-Radiance Recovery via Transient Event Frequency – Supplementary Material –

Jin Han[1,2] Yuta Asano[2] Boxin Shi[† 3,4] Yinqiang Zheng[1] Imari Sato[1,2]

[1]Graduate School of Information Science and Technology, The University of Tokyo [2]National Institute of Informatics

[3]National Key Laboratory for Multimedia Information Processing, School of Computer Science, Peking University

[4]National Engineering Research Center of Visual Technology, School of Computer Science, Peking University

{jinhan, asanoy, imarik}@nii.ac.jp shiboxin@pku.edu.cn yqzheng@ai.u-tokyo.ac.jp

7. Time Bounds for Frequency and Integration

7.1. Time bounds comparison

The time bounds selection is a key difference between the integration-based method and our proposed frequency-based method. As shown in Fig. 13, the starting time bounds (t_s, labeled with blue star) are identical for both methods. But the ending time bounds for frequency (t_e^{freq}, labeled with red star) and integration (t_e^{inte}, labeled with green star) are different according to their definitions. For event integration, radiance values are computed based on the number of triggered events. Therefore, so we count the number of events until the light becomes constant. In contrast, for event frequency, since we focus on the period when events are triggered in a constant frequency, the ending time bound is earlier than that of integration. Take patch "a" and "e" in the ColorChecker for comparison, we can find that t_e^{inte} is much later than t_e^{freq} in the darker patch (*i.e.*, patch "e"), which will introduce more noise for integration of events. By intercepting the period with constant TEF, the radiance values recovered from frequency of events are more robust and stable, especially in darker area of a scene or low-light conditions.

7.2. Time bounds detection

The starting time bounds t_s and ending time bounds t_e^{freq} can be easily detected by checking the time interval. Specifically, for t_s, when the time interval between two consecutive events is smaller than a pre-defined threshold, it indicates that the light is turned on at this time stamp. For t_e^{freq}, when the time interval changes over the pre-defined threshold, it means that the lighting becomes constant. The thresholds can be chosen based on the characteristics of the event camera and the lighting conditions. We can change the thresholds to adjust the range intercepted for constant event frequency by increasing or decreasing the thresholds.

† Corresponding author

Project page: https://github.com/hjynwa/TEF

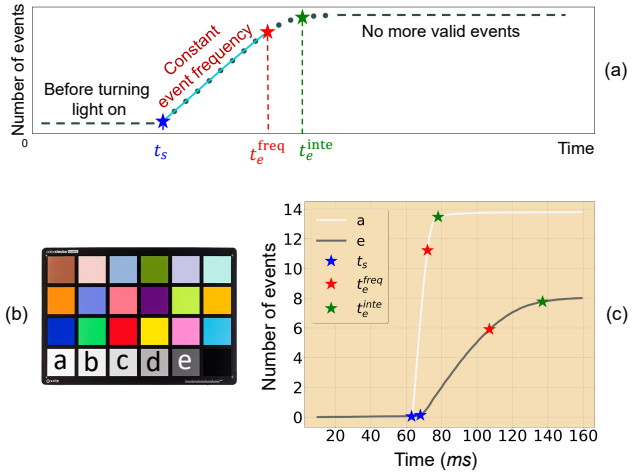

Figure 13. (a) The number of events changes along time when turning on a light. There exists a period when events are triggered in a constant frequency. (b) The MacBeth ColorChecker. (c) The curves of patch "a" and "e" labeled with t_s, t_e^{freq}, and t_e^{inte} are selected for comparison.

Please refer to our project page for implementation details.

8. More Experimental Results

We provide more experimental analysis and results to demonstrate the fidelity of the radiance recovered from the proposed TEF.

8.1. Hyperspectral imaging

By applying the narrow-band light spanning the wavelengths of interest, we can reconstruct the spectral curve of each point in a painting. The ground truth of spectral curves can be measured by a spectrometer with an fiber optical detector. As shown in Fig. 14, we measure the ground truth of spectral curve of a point, and compare it with our frequency-based estimation. In this figure, the spectral curves of the points indicated by yellow boxes are similar to the ground truth curves. We also provide additional image relighting

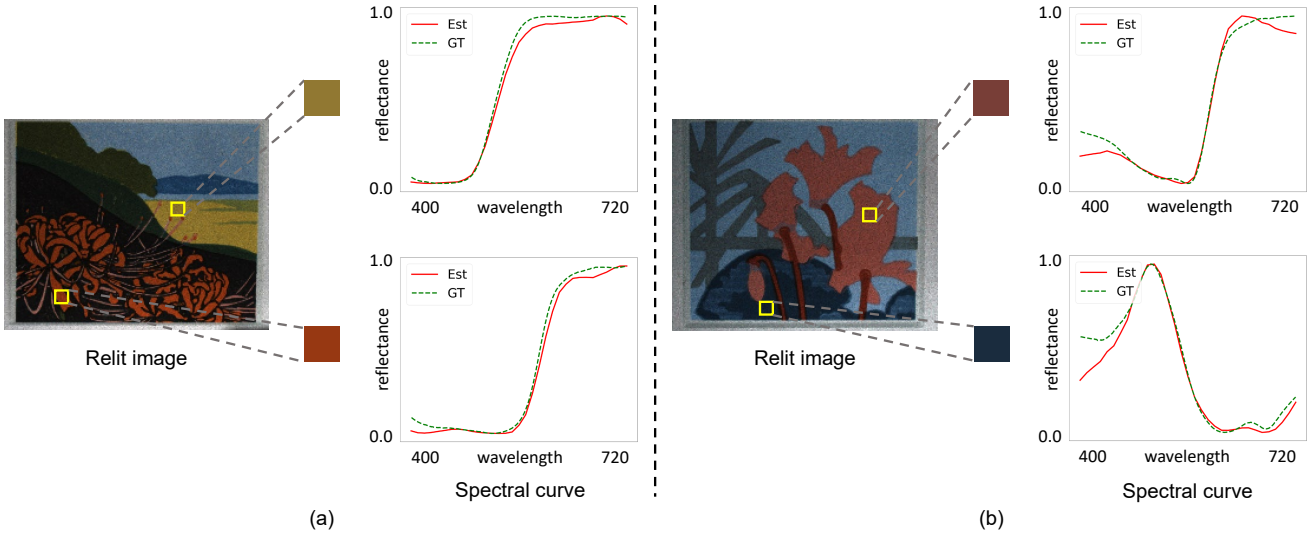

Figure 14. Two examples of spectral curve reconstruction. The points selected are enlarged and labeled with yellow boxes. The curves show the similarity between our estimation (red solid line labeled as "Est") and the ground truth (green dotted line labeled as "GT").

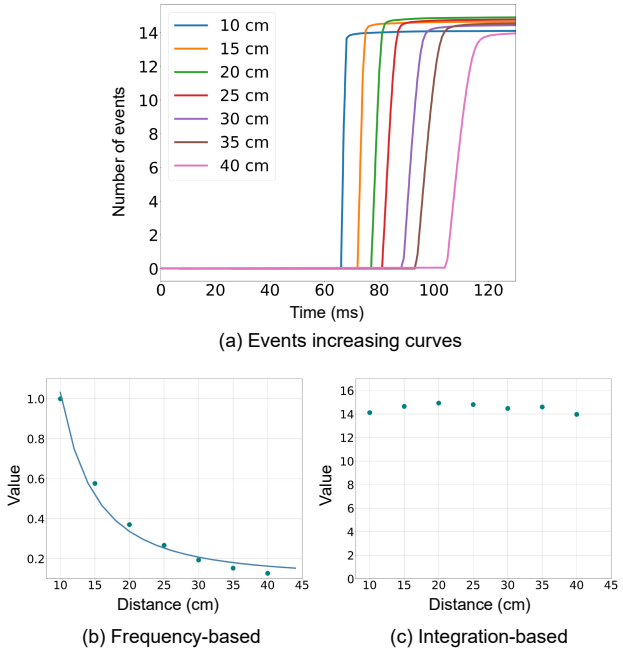

Figure 15. (a) The events increasing curves of settings with lights in different distances. (b) The relationship between transient event frequency and distance. (c) The relationship between integration of events and distance.

results in Fig. 16 and Fig. 17.

8.2. Depth sensing

The transient event frequency can be used for depth sensing, as validated by the inverse square law of light fall-off property described in Eq. (10). In Fig. 15 (a), we measure the number of events and plot events increasing curves of settings with lights at different distances. Based on these curves, we provide graphs showing distances on the horizontal axis and values recovered by our frequency-based and integration-based approaches in Fig. 15 (b) and (c). It is obvious that there are small differences among the number of integrated events of different settings. Thus, the integration-based approach cannot accurately provide the change in radiance with distance, making it difficult to estimate the distance information in a scene. In contrast, the values recovered by the frequency-based approach clearly follow the inverse square law of light shown in the solid line in Fig. 15 (b). This comparison demonstrates the superiority of the frequency-based method on distinguishing the small difference of radiance values.

Depth estimation results of several scenes are shown in Fig. 18. By comparison, we can find that the depth information from an image captured by a conventional RGB camera are easily affected by the exposure time. In the first case of Fig. 18, the near two layers suffer from saturation (over-exposure), which makes them hard to distinguish. In contrast, our frequency-based method is not affected by exposure effect due to the HDR property of event cameras. The integration baseline cannot clearly distinguish layers at different distances.

8.3. Iso-depth contour reconstruction

The comparisons on iso-depth contour reconstruction are shown in Fig. 19. The iso-depth contour maps reconstructed from the integration baseline have lower resolution of radiance values, making it difficult to cluster different points at the object surface into the iso-depth contours. The iso-depth contours recovered by TEF are clear, which is helpful in detecting the shape of the objects.

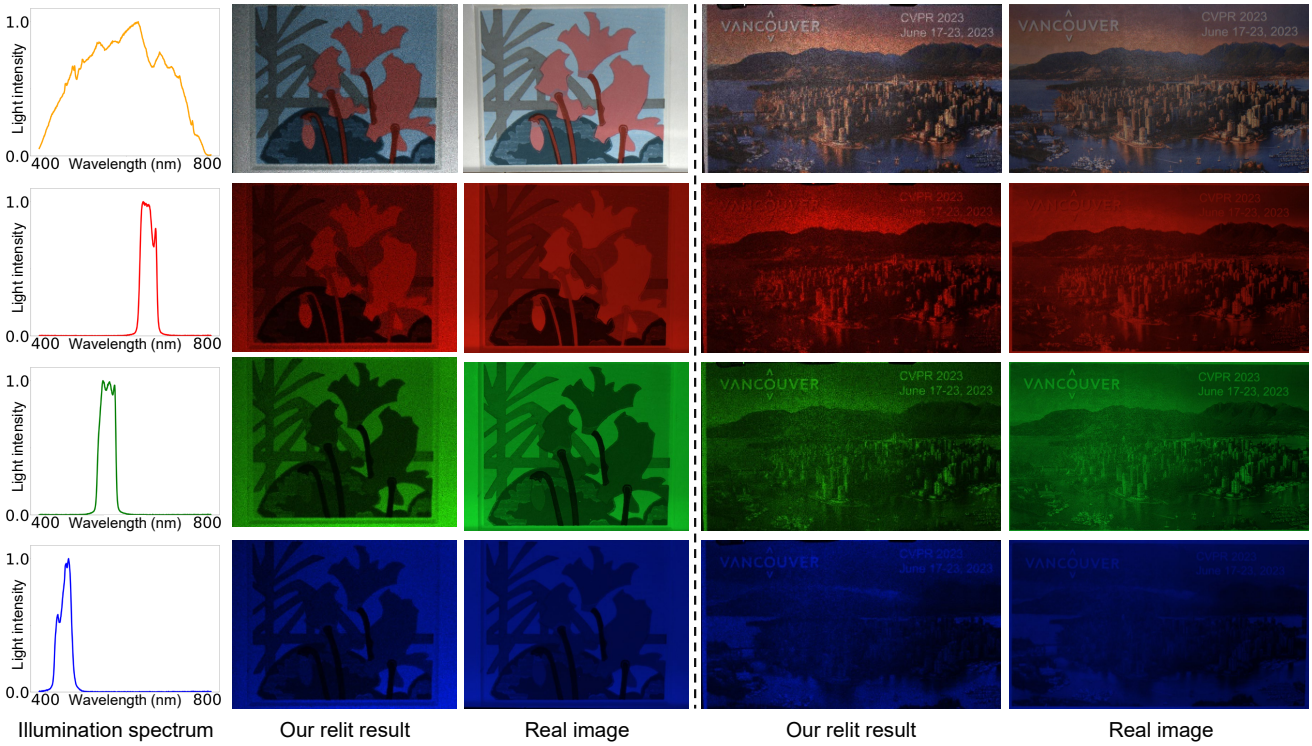

Figure 16. Image relighting results group 1. The relit images are computed from the recovered spectral reflectance curves under 4 different illuminations. The illumination spectrums are measured by a spectrometer. The real images are captured using an RGB camera.

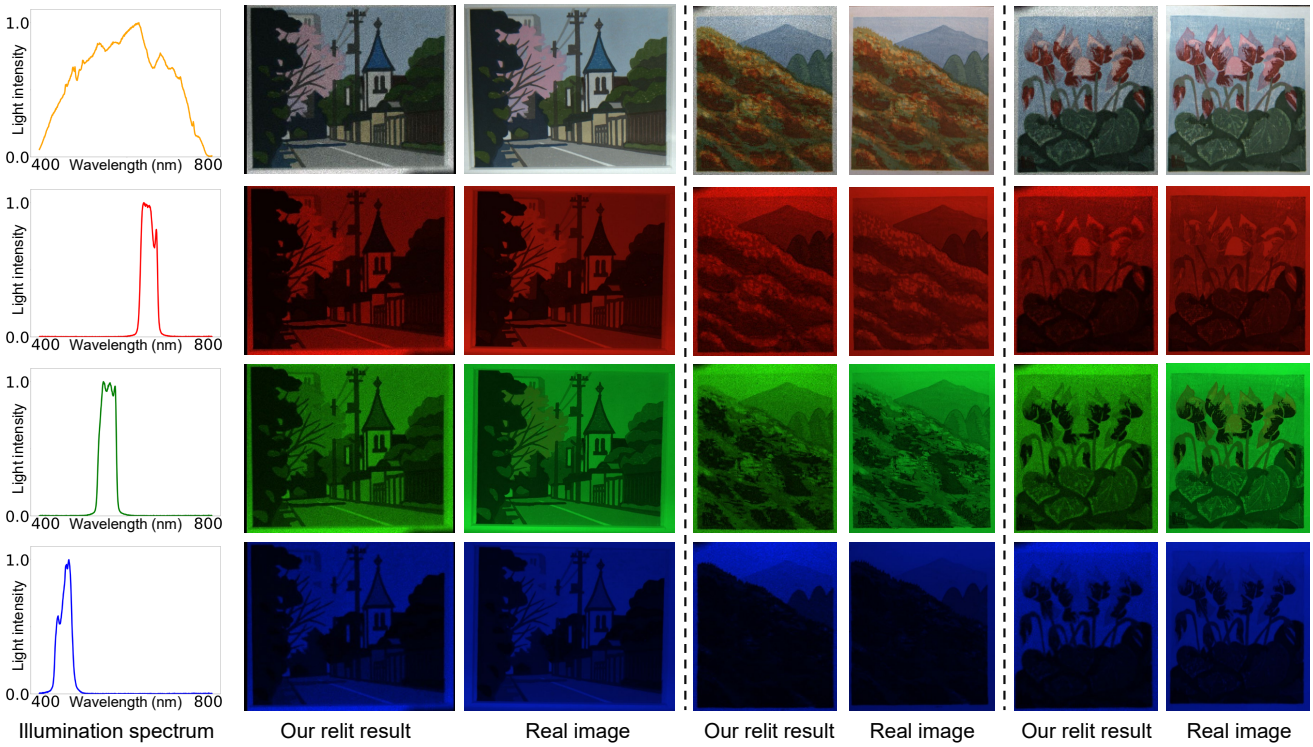

Figure 17. Image relighting results group 2. The relit images are computed from the recovered spectral reflectance curves under 4 different illuminations. The illumination spectrums are measured by a spectrometer. The real images are captured using an RGB camera.

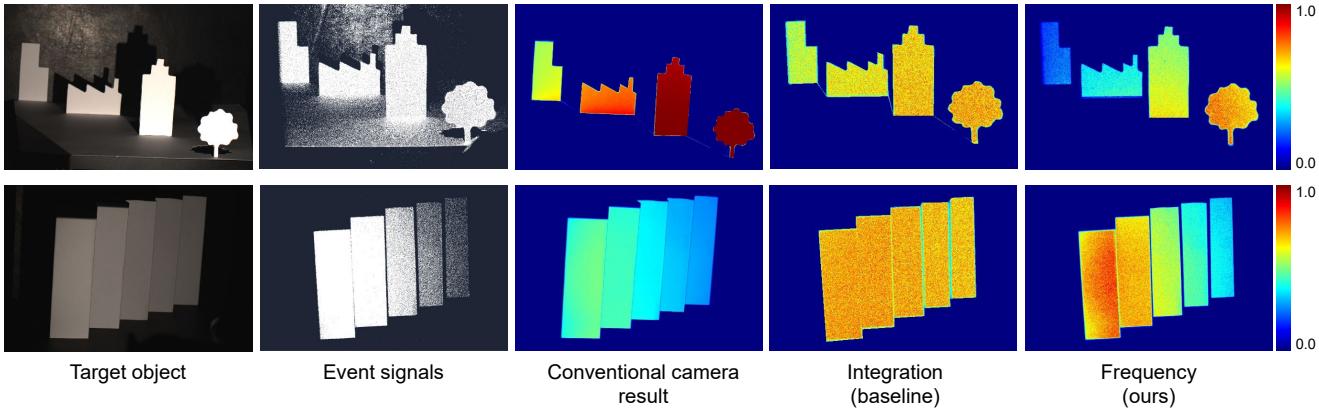

Figure 18. Depth map results comparison. The left 2 columns are raw data captured by a conventional camera and an event camera, respectively. The right 3 columns are depth map results from the conventional camera, the integration of events baseline, and our frequency-based method, respectively.

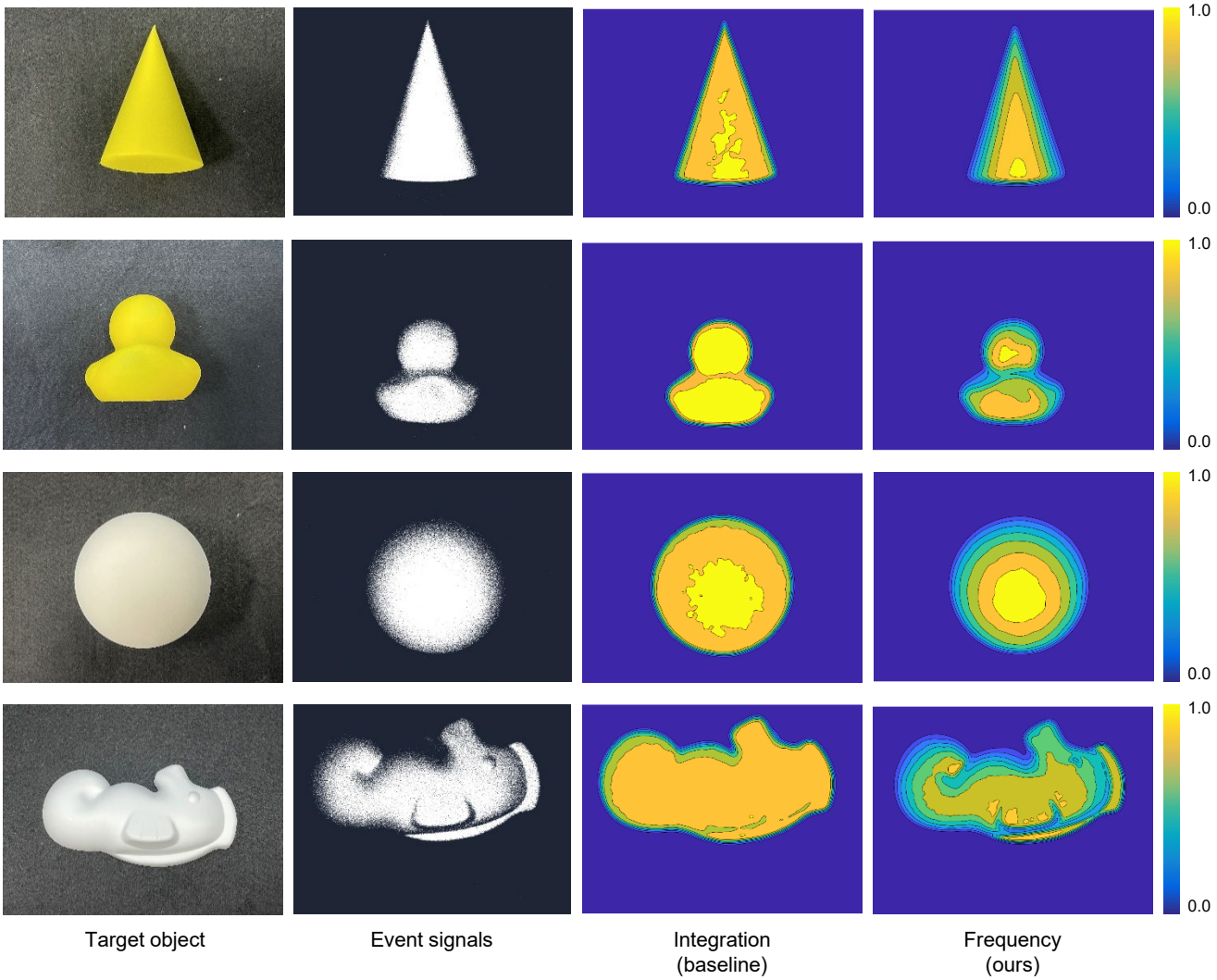

Figure 19. Iso-depth contour results comparison. From left to right columns are target objects captured by a conventional camera, the event signals, and the iso-depth contour reconstruction from integration of events baseline and our frequency-based method.